Cold-cavity measurement of optical loss from oxide-confined vertical-cavity surface-emitting lasers

Stewart T. M. Fryslie,[a] Dominic F. Siriani,[b] and Kent D. Choquette
Department of Electrical and Computer Engineering, University of Illinois, Urbana, Illinois 61820, USA

(Received 17 November 2013; accepted 18 February 2014; published online 10 March 2014)

Microcavity laser design and performance optimization requires a quantitative knowledge of the cavity optical losses. A generalized method using sub-threshold spectral measurements matched to model calculations is demonstrated to determine optical loss in microcavity lasers. Cold-cavity spectral characteristics are used to extract the size-dependent optical loss for small diameter oxide-confined vertical-cavity surface emitting lasers. For oxide aperture diameters less than 4 μm, the oxide scattering loss can be greater than 10 cm^{-1}, similar to the typical values of free carrier absorption loss. © *2014 AIP Publishing LLC*. [http://dx.doi.org/10.1063/1.4868038]

Microcavity lasers and other devices composed of optical microcavities are critical components in photonic technologies. Optical microcavities are important for a number of applications, such as cavity quantum electrodynamics,[1] enhancement, and suppression of spontaneous emission through the Purcell effect,[2] novel light sources, dynamic filters in optical communication, as well as soliton,[3,4] and chaos[5] effects in quantum-well microcavities.[6] Semiconductor microcavity lasers such as vertical-cavity surface-emitting lasers (VCSELs) benefit from modified lasing characteristics resulting from small cavity volume, high modulation bandwidth, single longitudinal mode emission, and low-power operation with very low threshold as a result of few optical modes interacting with the optically active material in the cavity. The demand for improved performance as well as ever-increasing levels of photonic integration drives further research in the design and performance optimization of microcavity lasers.

Microcavity laser design and performance optimization require a quantitative knowledge of the laser gain and losses. The modal gain required to reach threshold is

$$\Gamma g_{th} = \alpha_i - \frac{1}{2L} ln(R_1 R_2), \tag{1}$$

where Γ is the mode confinement factor, L is the cavity length, R_1 (R_2) is the top (bottom) mirror reflectivity, and α_i is the intrinsic optical loss of the cavity.[7] The mirror loss from the second term in (1) is often known from the device structural design such as the composition of the layers and the number of periods in distributed Bragg reflector mirrors. The intrinsic loss α_i is less straightforward to determine and contains both cavity-size independent (such as free carrier absorption) and dependent contributions (such as scattering and diffraction from transverse optical confinement).

The size-dependent optical loss for VCSELs has previously been determined by analysis of the external quantum efficiency[8,9] or threshold voltage.[10] These approaches, however, require lasing operation, in which thermal effects can obscure scattering loss, the latter of which can dominate for small cavity diameters. Sophisticated simulation packages may also be used to extract the loss from exact modeling to match experimental VCSEL performance, but this is not conducive to rapid device design and evaluation. A simple method to directly extract size-dependent optical loss from cold-cavity measurements will aid in the design and characterization of VCSELs and other microcavity lasers.

Sub-threshold spectral characterization combined with a Helmholtz waveguide model incorporating complex refractive index has previously been used to characterize optical loss in photonic crystal VCSELs.[11] By extracting the modal loss from observed spectral-mode splitting, it was shown that the optical scattering loss contributes significantly to the transverse optical confinement and supported modes. This procedure is a general result that is not specific to the photonic crystal VCSEL structure, and so it should be applicable to any microcavity laser structure. Here, we demonstrate this semi-empirical technique to analyze the cavity-size dependent optical scattering loss of small diameter oxide-confined VCSELs, which are widely deployed for short-range optical interconnects.

Driven by the ever increasing performance requirements of optical interconnects in data center and computing applications, data transmission bandwidth are required to increase at simultaneously lower power consumption and narrower spectral width.[12,13] These demands tend to promote small diameter oxide-confined VCSELs, which, however, do not exhibit properties that scale linearly with the size of the device.[10,14,15] Knowledge of the size-dependent optical loss will continue to be valuable in designing small cavity VCSELs.

To perform the optical loss analysis, we reduce our VCSEL structure to a simple cylindrical optical waveguide model where the region within the lasing aperture corresponds to the high index guiding core and the region above and below the surrounding buried oxide layer is the cladding. To introduce loss created by the buried oxide layer, we use a complex refractive index in the cladding region.[16] The laser modes can be obtained from solutions to the scalar Helmholtz equation given by[11]

$$\nabla^2 U(r,\phi,z) + n^2(r) k^2{}_0 U(r,\phi,z) = 0, \tag{2}$$

[a]Electronic mail: fryslie2@illinois.edu. Tel.: 714-225-1524.
[b]Present address: MIT Lincoln Laboratory, Lexington, Massachusetts 02420, USA.

with solutions given by

$$U(r,\phi,z) = u(r)e^{il\phi}e^{i\beta z}, \tag{3}$$

where U is the field profile, n is the refractive index profile, k_0 is the wavenumber, l is an integer, and β is the real-valued propagation constant assumed to be equal to $2\pi/L$, where L is the longitudinal cavity length. Inserting (3) into (2) and taking a finite-differences approach to facilitate more easily an iterative fit to experimental data gives the eigenvalue problem

$$\left[\frac{u_{j+1}-2u_j+u_{j-1}}{(\Delta r)^2}+\frac{1}{r_j}\frac{u_{j+1}-u_{j-1}}{2\Delta r}-\left(\beta^2+\frac{l^2}{r_j^2}\right)u_j\right] = -n_j^2k_0^2u_j, \tag{4}$$

where j is an index associated with a point in space. The parameters that determine the solutions to (4) are the refractive index of the core, n_{core}, and complex cladding refractive index, $n_{clad} = n'_{oxide} + in''_{oxide}$. By inclusion of a complex refractive index for the cladding region in solving for the cavity modes, we obtain complex wavenumbers, k_0, from which the real valued resonances, λ_0, can be calculated by $\lambda_0 = 2\pi/Re\{k_0\}$ and the field amplitude loss, α_i, can be extracted by $\alpha_i = \mathrm{Im}\{k_0\}$. Note that a complex wavenumber k_0 in (2) defines a wave that resonates (the real part) and decays (the imaginary part), as is appropriate for an optical cavity.

The real values n_{core} and n'_{oxide} can be calculated from the transmission matrix method[7] using the VCSEL epitaxial parameters, and then can be used to solve for the fundamental and first higher-order mode resonances, λ_{01} and λ_{11}, respectively. The imaginary term in the complex cladding refractive index is then added and used to fit this model to experimental measurements, meaning that we find the value n''_{oxide} giving mode resonances with spectral splitting, $\Delta\lambda = \lambda_{01} - \lambda_{11}$, equal to that of experimentally collected sub-threshold spectral data. Note that the calculation is sensitive to the difference $\Delta n_{real} = n_{core} - n'_{oxide}$, rather than the specific values of n_{core} and n'_{oxide}, and we further reduce the significance of uncertainties of the refractive index values in our experimental method described next.

The devices under investigation are oxide-confined VCSELs with aperture diameter varying by 0.5 μm increments for the characterization of size-dependent optical scattering loss. The lasers operating nominally at 850 nm contain multiple GaAs quantum wells with 23 top distributed Bragg reflector mirror periods and a 30 nm thick high aluminum content layer in the period nearest the optical cavity, all grown by metal organic chemical vapor deposition.

In our experimental procedure, we first measure the light output vs. current characteristics of the VCSELs using a semiconductor parameter analyzer. Shown in Fig. 1 is the threshold current and threshold current density as a function of oxide aperture size. Aperture scattering loss is significant for small diameter VCSELs but insignificant for broad area VCSELs due to less interaction between the electric field of the laser modes and oxide aperture.[10] As shown in Figure 1, threshold current density scales approximately linearly with the cavity size until the aperture scattering loss and concomitant leakage current become significant.[10] For this set of

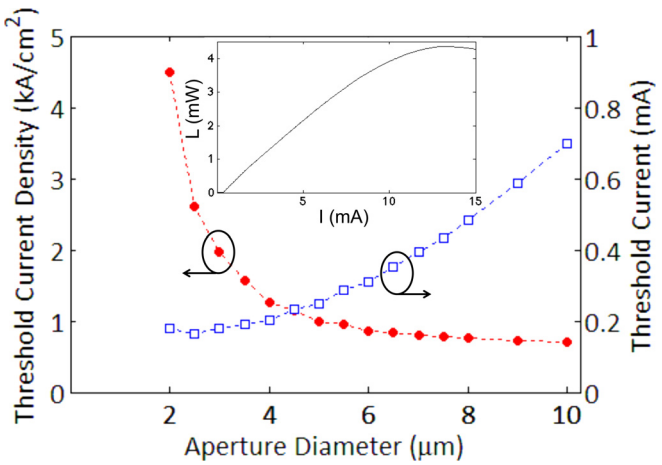

FIG. 1. Threshold current and current density versus oxide aperture size. The inset shows measured light intensity versus bias current for VCSEL with 6 μm aperture.

lasers, the smallest VCSEL with linearly scaling threshold current density has an aperture diameter of 6 μm. Therefore, the 6 μm oxide aperture VCSEL is considered to have vanishing aperture scattering loss, while all smaller devices have an additional size-dependent loss.

We use an optical spectrum analyzer to obtain the necessary cold-cavity spectral measurements. The spectral splitting between the fundamental and first higher-order mode is measured, as shown in Figure 2, for each VCSEL biased at an injection current of approximately 0.9 times threshold in order to avoid thermal effects. Using the spectral splitting of the smallest device, for which threshold current density scales linearly with aperture size, we solve Eq. (4) for the value of Δn_{real} that yields an equivalent $\Delta\lambda$ for a lossless aperture (i.e., with no imaginary n''_{oxide} term in the calculation). Using this new value of Δn_{real} in our loss calculations, we extract the additional optical loss for the smaller diameter VCSELs, which reduces the impact of uncertainty for the real refractive indices, mentioned previously. The calculated results for the excessive fundamental mode loss due to aperture scattering are shown in Figure 3. The calculated loss from the oxide cladding region of the small diameter

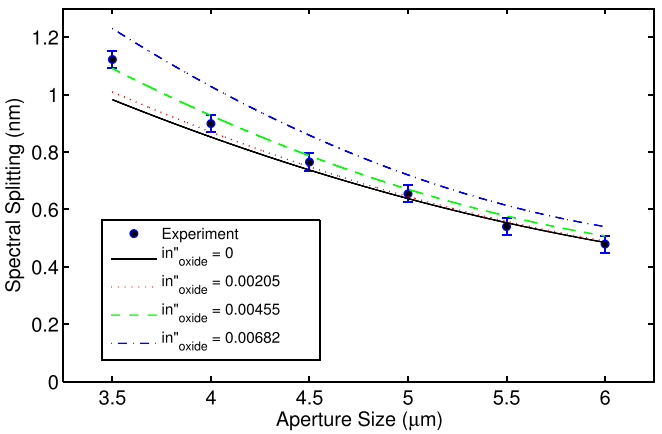

FIG. 2. Plot of measured subthreshold spectral splitting between fundamental and first higher-order mode as function of aperture size with error bars corresponding to the 0.06 nm resolution of the optical spectrum analyzer. The curves are calculated from Eq. (4), for varying values of n"$_{oxide}$ equal to 0, 5, 10, and 15 cm^{-1} for the 3.5 μm aperture VCSEL.

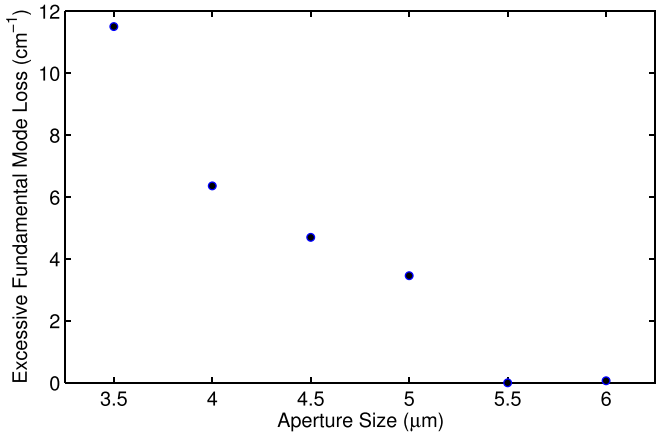

FIG. 3. Oxide optical loss obtained from matching cold-cavity spectra to model calculations (Eq. (4)) as a function of aperture size.

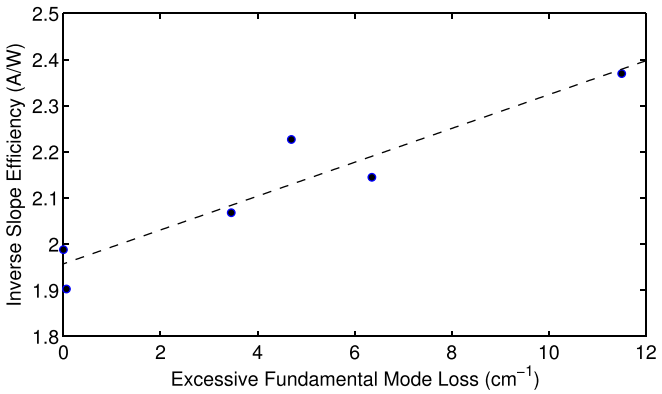

FIG. 4. The inverse measured VCSEL slope efficiency versus the oxide optical loss.

VCSELs increases with decreasing aperture size as expected. Furthermore, optical loss α_i is correlated to the laser slope efficiency, η_{slope}, by the proportionality $\eta_{slope} \propto \alpha_m/(\alpha_i + \alpha_m)$, where α_m is the mirror loss. Figure 4 reveals that the calculated optical scattering loss is inversely proportional to experimental measurements of the laser slope efficiency for corresponding devices, as expected.

In conclusion, we have demonstrated an analysis of cavity-size dependent optical scattering loss in oxide confined VCSELs using cold-cavity spectral measurements. We have shown that the results of our analysis correspond well with theory and other laser characteristics such as threshold current density and laser slope efficiency. We find that the scattering loss obtained for smaller lasers exceed $10\,\mathrm{cm}^{-1}$, which is of the order of typical values of free carrier absorption loss for microcavity laser diodes such as VCSELs. Our analysis procedure is thus shown to be appropriate for microcavity lasers; this should also prove to be a general applicable technique for other microcavity or even nanocavity laser systems as long as an appropriate optical model is used for matching the spectral characteristics.

This work was supported by the National Science Foundation under Award Number DMI 0328162.

[1]Y. Yamamoto, F. Tassone, and H. Cao, *Semiconductor Cavity Quantum Electrodynamics* (Springer, Berlin, 2000).
[2]E. M. Purcell, Phys. Rev. **69**, 37 (1946).
[3]V. B. Taranenko and C. O. Weiss, IEEE J. Sel. Top. Quantum Electron. **8**, 488 (2002).
[4]S. Barland, J. R. Tredicce, M. Brambilla, L. A. Lugiato, S. Balle, M. Giudici, T. Maggipinto, L. Spinelli, G. Tissoni, T. Knödl, M. Miller, and R. Jäger, Nature **419**, 699 (2002).
[5]A. D. Stone, Phys. Scr. **T90**, 248 (2001).
[6]G. Khitrova, H. M. Gibbs, F. Jahnke, M. Kira, and S. W. Koch, Rev. Mod. Phys. **71**, 1591 (1999).
[7]L. A. Coldren, S. W. Corzine, and M. L. Mashanovitch, *Diode Lasers and Photonic Integrated Circuits* (Wiley, Hoboken, 2012).
[8]B. J. Thibeault, T. A. Strand, T. Wipiejewski, M. G. Peters, D. B. Young, S. W. Corzine, L. A. Coldren, and J. W. Scott, J. Appl. Phys. **78**, 5871 (1995).
[9]T. H. Oh, D. L. Huffaker, and D. G. Deppe, Appl. Phys. Lett. **69**, 3152 (1996).
[10]K. D. Choquette, W. W. Chow, G. R. Hadley, H. Q. Hou, and K. M. Geib, Appl. Phys. Lett. **70**, 823 (1997).
[11]D. F. Siriani, P. O. Leisher, and K. D. Choquette, IEEE J. Quantum Electron. **45**, 762 (2009).
[12]M. P. Tan, S. T. M. Fryslie, J. K. Guenter, J. A. Tatum, R. H. Johnson, and K. D. Choquette, Electron. Lett. **49**, 612 (2013).
[13]M. P. Tan, S. T. M. Fryslie, J. A. Lott, N. N. Ledentsov, D. Bimberg, and K. D. Choquette, IEEE Photonics Technol. Lett. **25**, 1823 (2013).
[14]E. R. Hegblom, D. I. Babic, B. J. Thibeault, and L. A. Coldren, Appl. Phys. Lett. **68**, 1757 (1996).
[15]B. J. Thibeault, E. R. Hegblom, P. D. Floyd, R. Naone, Y. Akulova, and L. A. Coldren, IEEE Photonics Technol. Lett. **8**, 593 (1996).
[16]A. E. Siegman, J. Opt. Soc. Am. A **20**, 1617 (2003).